

Analysis of the long-lived slepton next-to-lightest supersymmetric particle in the gauge-mediated supersymmetry breaking model at a linear collider

Pedro G. Mercadante

Department of Physics, Florida State University, Tallahassee, Florida 32306

J. Kenichi Mizukoshi and Hitoshi Yamamoto

Department of Physics and Astronomy, University of Hawaii, Honolulu, Hawaii 96822

(Received 16 November 2000; published 30 May 2001)

We performed an analysis on the detection of a long-lived slepton at a linear collider with $\sqrt{s} = 500$ GeV. In gauge-mediated symmetry breaking models a long-lived NLSP is predicted for a large value of the supersymmetry breaking scale \sqrt{F} . Furthermore in a large portion of the parameter space this particle is a stau. Such heavy charged particles will leave a track in the tracking volume and hit the muonic detector. In order to disentangle this signal from the muon background, we explore the kinematics and particle identification tools: a time-of-flight device, dE/dX , and Cherenkov devices. We show that a linear collider will be able to detect long-lived staus with masses up to the kinematical limit of the machine. We also present our estimation of the sensitivity to the stau lifetime.

DOI: 10.1103/PhysRevD.64.015005

PACS number(s): 14.80.Ly, 11.30.Pb, 13.85.Qk

I. INTRODUCTION

In many supersymmetric models charged long-lived particles can exist. In models with R -parity violation, this happens when the lightest supersymmetric particle (LSP) is a slepton and the R -parity violation term is small [1]. Another class consists of models where the LSP is not the usual [such as in minimal supergravity (MSUGRA)] $U(1)_Y$ gaugino but rather a $SU(2)$ gaugino; in this case the next-to-lightest supersymmetric particle (NLSP) is the lightest chargino, almost degenerate in mass with the neutralino LSP, and will decay after traveling centimeters or meters into the LSP plus a soft lepton or pion [2]. This type of model arises rather naturally in the anomaly mediated supersymmetry (SUSY) breaking scenario [3]; however, in this scenario the mass splitting is typically larger than the pion mass, leading to decay length of the order of $c\tau \sim 10$ cm at most. Another class of models where long-lived charged particles occur is in gauge-mediated supersymmetry breaking (GMSB) models [4,5]. Depending on the value assumed for the SUSY breaking scale, \sqrt{F} , the gravitino is the LSP. Moreover, because of the weak coupling of the gravitino to the SUSY fields, the NLSP could in principle be a long-lived massive particle. Throughout this paper we will concentrate on the detection of long-lived charged particles in the GMSB framework. The techniques presented, however, are applicable to general nonstrongly interacting heavy long-lived charged particles.¹

In GMSB an intermediate sector is responsible for communicating supersymmetry breaking to the MSSM sector. In these models the gravitino mass is given by

$$M_{\tilde{G}} = \frac{F}{\sqrt{3}M_{\text{pl}}} = \left(\frac{\sqrt{F}}{100 \text{ TeV}} \right)^2 2.37 \text{ eV}, \quad (1)$$

where M_{pl} is the reduced Planck mass. For the $\sqrt{F} \sim 100$ TeV (to be compared with 10^{11} GeV, a typical MSUGRA value of SUSY breaking scale), $M_{\tilde{G}} \sim \text{eV}$, making the phenomenology quite interesting.

Moreover, because of the very weak interaction of the gravitino, all supersymmetric particles will decay into the NLSP and this will decay into the gravitino (which will escape detection) and its standard model partner. Thus the nature of the NLSP and its decay length will play a fundamental role in the phenomenology of the model. Because soft terms in GMSB models are generated by the gauge couplings, the NLSP is usually either a neutralino or a stau. Many phenomenological studies have been made for the Fermilab Tevatron and CERN e^+e^- collider LEP in the context of this model [7–9]. More recently some studies for the CERN Large Hadron Collider (LHC) and run II at Tevatron also have been addressed [10,13,14]. For the Next Linear Collider (NLC) the case for a neutralino NLSP, both long- and short-lived, was considered by Ambrosanio [15] and the case for a stau NLSP with prompt decay was considered by Kanaya [16].

In this work we improve over our previous analyses [16,17] in the search for a long-lived stau at NLC, presenting here our estimations for a lifetime measurement. In the GMSB the NLSP lifetime is given by

$$c\tau = 16\pi \frac{F^2}{M_{\text{NLSP}}^5} \sim \left(\frac{\sqrt{F}}{10^7 \text{ GeV}} \right)^4 \left(\frac{100 \text{ GeV}}{M_{\text{NLSP}}} \right)^5 10 \text{ km}. \quad (2)$$

From this expression, one can see that the measurement of the NLSP mass and lifetime will determine the value of the fundamental SUSY breaking scale \sqrt{F} . From perturbative arguments it is possible to set a lower limit in \sqrt{F} for the

¹In Ref. [6], the authors raise the issue of hadronization effects for color-triplet particles. Some of them will hadronize into neutral exotic mesons. In addition to that, the inelastic hadronic reactions can change the charge of the mesons.

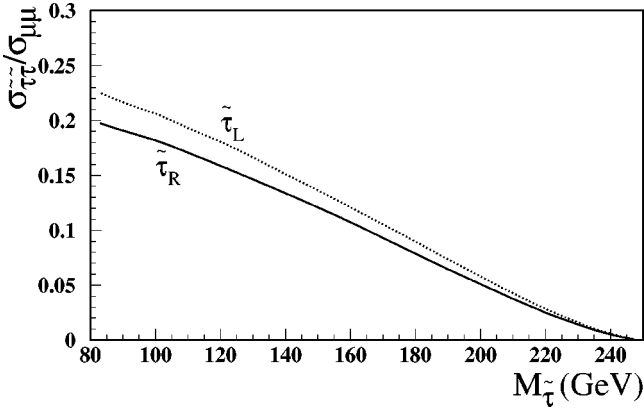


FIG. 1. Stau pair production cross section normalized by muon pair as a function of stau mass in $\sqrt{s}=500$ -GeV linear collider. The full (dotted) line is for the right- (left-)handed stau pair.

complete set of parameters in the GMSB framework. Nevertheless, for the range of stau masses under consideration, it is always possible to find parameters which give a $c\tau \sim \mu\text{m}$. On the other hand, there is no solid theoretical argument for an upper limit on \sqrt{F} . However, a LSP gravitino with mass higher than few keV is disfavored in some cosmological scenarios for over-closing the Universe [18]. This translates to roughly $\sqrt{F} \lesssim 3000$ TeV.

The rest of this paper is organized as follows. In Sec. II we describe our simulation using the program ISAJET [19] to generate stau pairs with the effects of a time-of-flight device, dE/dX , and a Cherenkov device to detect a heavy particle. In Sec. III we use the stau pair production process to extract limits on the lifetime of stau which leads to limits on the SUSY breaking scale in a GMSB model. In Sec. IV we present our conclusions.

II. SELECTION CRITERIA FOR STAU PAIR PRODUCTION

Stau pair production at a linear collider provides a clean search environment. Furthermore, the production cross section is model independent, depending only on the mass of the staus and on the mixing angle between the left- and right-handed superpartners. In Fig. 1 we show the pair production cross section (normalized to $\sigma_{\mu\mu}=450$ fb at $\sqrt{s}=500$ GeV) for the left- and right-handed states as a function of stau mass. The stau pair cross section is smaller than $\sigma_{\mu\mu}$ due to its scalar nature and it rapidly drops when we approach the kinematical limits of the accelerator. Nevertheless, we note that for masses around 240 GeV we still have a cross section of $\mathcal{O}(10)$ fb, which should be observable provided that the background is manageable.

We will first describe the selection criteria without particle identification which will be used in later sections to extend the range of sensitivity to the full beam energy. The signal we are looking for is a back-to-back track with corresponding hits in the muon chamber. With this requirement tracks from π , K , p , and e are removed. To reject the two photon process of $\gamma\gamma \rightarrow \mu^+\mu^-$, we note that the $\mu^+\mu^-$ pair in this process tends to have a low invariant mass and be

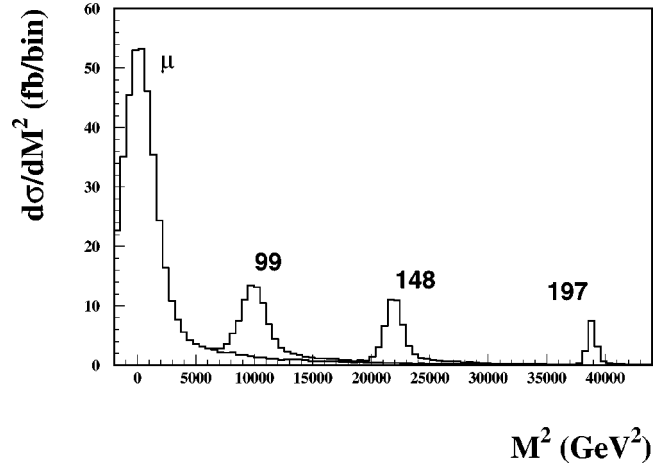


FIG. 2. The distribution of track mass square for muon and for several values of stau masses (in units of GeV, indicated by numbers on the top of peaks.)

boosted along the beam pipe. Thus we require the following cuts: (1) $\cos\theta < 0.8$, to guarantee good track quality; (2) $|p| > 0.5E_{\text{beam}}$; and (3) $|p_z^{\text{tot}}| < 0.25E_{\text{beam}}$, where θ is the angle between the initial electron and final negative charged particle, $|p|$ the absolute value of its momentum, and p_z^{tot} is the net momentum in the beam direction. Finally, E_{beam} is the beam energy. After these cuts, the two photon initiated muon pair production is estimated to be 1.4 fb. We are then left with muon pair production $e^+e^- \rightarrow \mu^+\mu^-$ as the main source of background.

In order to reduce the muon pair background we shall explore the heavy mass of the staus. In a e^+e^- collider the energy in the center of mass is fixed, so in a pair production process the energy of the final particles is also known. It is well known, however, that in a high-energy linear collider beamsstrahlung and initial-state radiation effects become important and the effective energy of the reaction is not fixed but presents a spectrum. In ISAJET, these effects have been implemented using the parametrization described in Ref. [20], where the radiation spectrum is well approximated by one photon emission from one of the initial state e^\pm . Assuming also that the direction of the emission is along the beam line, the mass estimate for each track in the laboratory frame is given by

$$M^2 = \left(\frac{\sqrt{\hat{s}}}{2\gamma} + \beta p_z \right)^2 - |p|^2, \quad (3)$$

$$\hat{s} = s(1 - |\Delta|), \quad (4)$$

$$\beta = \Delta / (2 - |\Delta|), \quad (5)$$

where $\Delta = p_z^{\text{tot}}/E_{\text{beam}}$, β is the boost parameter and $\sqrt{\hat{s}}$ is the center-of-mass energy of the two tracks.

In Fig. 2 is shown the cross section distribution as a function of M^2 which is estimated according to Eq. (3). In this plot we can see the muon distribution peaking at zero mass with a tail from beamsstrahlung. We also see the distribution

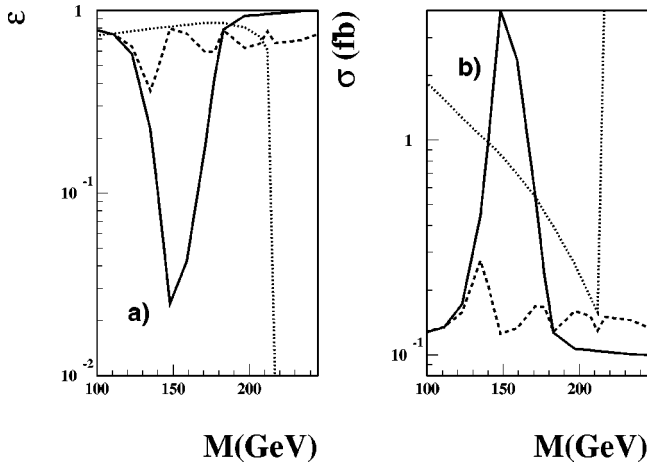


FIG. 3. (a) The efficiency for the signal. The dotted line is the efficiency for just kinematics cuts (cuts 1–4), the dashed line is for the time-of-flight cuts (cuts 1 and 5), and the solid line is for dE/dX cuts (cuts 1 and 6). (b) The reach in cross section for a linear collider with luminosity of 50 fb^{-1} . The dotted line is using just kinematics, the dashed line is using time of flight, and the solid line is using dE/dX .

of staus production for several values of masses. The momentum resolution is taken to be $\delta p_T/p_T = 5 \times 10^{-5} p_T$ (GeV), where p_T is the particle transverse momentum. Based in this plot we use the following cut: (4) $|M^2 - M_{\tilde{\tau}}^2| < 3000 \text{ GeV}^2$, where $M_{\tilde{\tau}}$ is a variable parameter in the search. The resulting efficiency after this cut is shown as the dotted line of Fig. 3(a). This is our basic strategy to reduce the muon background. To further improve the sensitivity, we study particle identification.

A. Time of flight

A time-of-flight (TOF) device can be used to identify heavy tracks. In our study we considered a linear collider with 1.4 ns of bunch separation. For a flight path length of $r=2$ m, the mean time of flight for a massless ($\beta=1$) particle is around 6.7 ns. In Fig. 4 we present the expected mean time delay as a function of mass. Assuming that we do not know which bunch crossing a given event is coming from, every 1.4 ns of TOF delay is consistent with the massless muon. We simulated the effect of a 50-ps error in the time-of-flight measurement, applying the following cut: (5) $\Delta t > 0.13$ ns, where Δt is the time-of-flight difference between a $\beta=1$ and a massive particle, modulo 1.4 ns.

This cut corresponds to about 2.5σ , so that about 1% of the muon background are kept. Applying this cut to both tracks we can relax cuts 2 and 3 and extend the mass range to the full beam energy. Notice that cut 2 restricts slepton mass to be $M_{\tilde{\tau}} \lesssim 216$ GeV. The efficiency of this cut as a function of mass is shown in Fig. 3(a) as the dashed line. The corresponding sensitivity is shown in Fig. 3(b). We see that for some values of the mass we have lower efficiency when the time delay with respect to $\beta=1$ case becomes equal to the bunch spacing. However, the efficiency is never below 0.3 because the actual path that the particle goes through de-

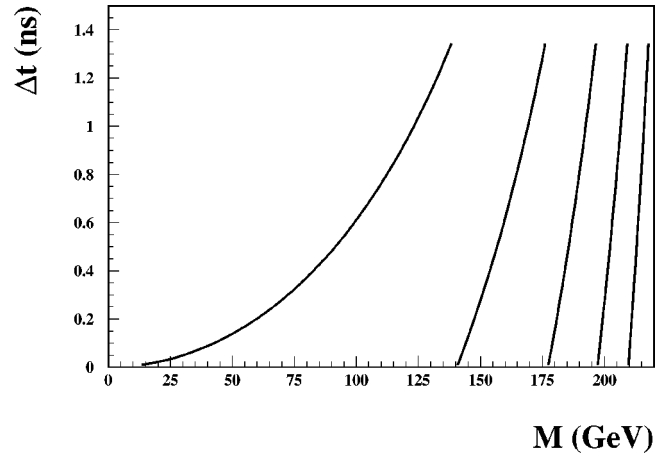


FIG. 4. The difference (modulo 1.4 ns for bunch ignorance) between muon time of flight and a massive particle as a function of mass for a path length of 2 m.

pends on the angle (the detector has cylindrical, but not spherical, symmetry): for each angle we have a different travel length.

B. dE/dX

When a charged particle goes through the detector it deposits energy by ionization. The amount of energy deposited, dE/dX , is a function of $\beta\gamma$ of the particle [21]. We assumed that the charged particle goes through argon and dE/dX has 5% resolution, which is a realistic value for a time projection chamber (TPC). To remove muons, we use the following cut: (6) $dE/dX - dE/dX(\text{muon})/\sigma(dE/dX) > 3$. The resulting efficiency is shown as the solid line in Fig. 3(a). We note a blind spot for masses around 150 GeV, where the energy deposited by a particle with $\beta\gamma \sim 1.3$ coincides with the one deposited by the muon, which has $\beta\gamma \sim \mathcal{O}(10^3)$. We also note that for lower value of $\beta\gamma$ (for masses below 150 GeV) dE/dX will give a unique value for $\beta\gamma$, thus knowing the momentum we can get the stau mass. As the figure shows, we can apply cut 6 to cover the high mass range up to the beam energy where the cuts 2 and 3 are not met.

In Fig. 3(b) we present, for each strategy, the minimum cross section (before cuts) that will be visible at a $\sqrt{s} = 500$ GeV linear collider with $L = 50 \text{ fb}^{-1}$. Our criteria are based on a three sigma significance; namely, $S \geq 3$ with $S = \epsilon\sigma\sqrt{L}/bg$, where σ is the signal cross section (before cuts), ϵ is the efficiency to pass the cuts, and bg is the expected background cross section after cuts. In addition, we require a minimum of five signal events after cuts.

A Cherenkov device can be used to measure $\beta\gamma$. With a device similar to the BABAR detector [22] it is possible to reject particles with $\beta\gamma > 8$. Cherenkov devices, however, in general have a large impact on the detector design due to its requirements on space and photon detection. If these requirements are met, a Cherenkov device can replace TOF or dE/dX discussed above.

A comment on the nature of our results is in order. We have presented a strategy based only on the pair production mechanism where particle identification had a relatively mi-

nor role to play. Nevertheless, in the models under consideration it is likely that other supersymmetric particles will be produced and end up in stau; in such decay chains the use of time of flight, dE/dX , and Cherenkov devices would play a critical role in identifying staus.² We also note that the results presented so far in Fig. 3 are rather independent of the model; it depends only on the pair production mechanism that will exist for any noncolored charged long-lived particle, provided that the cross section is not too small. The efficiency to pass the cuts depends only on the mass of the particle,³ so that Fig. 3 can be read in a model-independent way: we see the minimal cross section that would lead to an observable signal as a function of the mass of a long-lived charged particle, regardless of the nature of this particle.

III. STAU DECAY LENGTH

Up to this point we supposed that the stau does not decay within the detector; however, as mentioned earlier, the lifetime can be viewed as a free parameter of the model. We will now discuss a simple measurement of the stau lifetime using the mode $e^+e^- \rightarrow \tilde{\tau}^+ \tilde{\tau}^-$. The case of a short-lived stau is to be studied elsewhere.

In order to ensure good measurement of momentum and dE/dX we require that each event should have one central track longer than 1 m, using the mass cut 4 to select tracks consistent with a heavy particle. We believe that such events will be essentially background free: a well reconstructed track, consistent kinematically with a heavy particle, regardless of the decay pattern.

One way to estimate the lifetime is to consider the number of events that decay before and after a certain length. With this method the error in the lifetime is given by

$$\frac{\sigma_{c\tau}}{c\tau} = \frac{1}{\sqrt{N}} \frac{\sqrt{R}}{\log(1+R)}, \quad (6)$$

$$R = \frac{N_1}{N_{\text{inf}}}, \quad (7)$$

where N_1 is the number of particles that decays between distance l_1 and l_2 , N_{inf} is the number of particles that decays after distance l_2 , and $N = N_1 + N_{\text{inf}}$ is the total number of particles that decay after distance l_1 . In practice, $l_1 = 1$ m, and l_2 is chosen such that the statistical power is maximized, which is found to occur at $R = 3.9$, but not exceeding the outer radius of the tracking volume. When the lifetime is short enough the optimum value of l_2 occurs within the tracking volume, and the error [Eq. (6)] is given by $1.24/\sqrt{N}$. On the other hand, a large lifetime may lead to the optimum

²The kinematical distribution, as proposed here, would be of no use in a process other than pair production.

³There is a model-dependent part in the angular distribution of the cross section that will have an effect in cut 1. But we note that the effect of this cut is small. One can also read Fig. 3 as the minimum cross section in the central region that will be observed at the NLC.

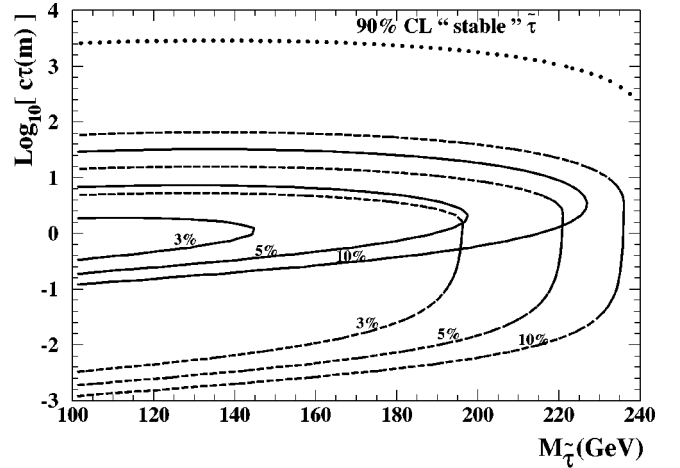


FIG. 5. Contours of constant error $\sigma_{c\tau}$ on the measurement of $c\tau$. The solid lines stand for the case $l_1 = 1$ m and the dashed lines are for $l_1 = 0.01$ m. The dotted line on the top of the figure indicates at 90% C.L. the case stau is stable up to the detector.

l_2 outside of the tracking volume in which case the error is approximately $1/\sqrt{N_1}$. In both cases the relevant quantity to get a precise measurement of the lifetime is the number of particles that decay inside the detector.

In Fig. 5, the solid lines represent the contour plot of the lifetime resolution as a function of the stau mass and lifetime where minimum track length (l_1) of 1 m is required. In the case of a short decay length it is not possible to reconstruct the stau track. However, one still can identify $\tilde{\tau}$ from the decay product of τ based on displaced vertex, as performed by DELPHI experiment at LEP II [11]. For the NLC small detector design the impact parameter resolution is expected to be $4.5 \mu\text{m} + 5.5 \mu\text{m}/(p \text{ GeV} \sin^{3/2}\theta)$ [12], a performance better than the DELPHI vertex detector. In order to take these cases into account, we also show the lifetime resolution for $l_1 = 1$ cm (the dashed lines). We see from this plot that in the optimistic case we would be able to measure the lifetime with a 10% precision as long as $c\tau$ is lower (bigger) than ~ 40 m (~ 0.01 m), for masses up to 200 GeV. A comparison with the CERN LHC is in order [13]. In this study Ambrosanio *et al.* show the capability of the CERN LHC to measure the stau lifetime in several models within the GMSB context. Their numbers are parameter space dependent as all possible reactions (that end in staus at the end of the decay chain) are used to extract the stau lifetime. It is of fundamental importance for the LHC to consider all possible reactions in order to get enough statistics. Their analysis shows that for models that give $M_{\text{stau}} \sim 100$ GeV they are able to get 10% precision (in a somewhat optimistic case) for $1 < c\tau$ (m) < 50 . Our analysis involves only the stau pair production, being essentially model independent.⁴ For $M_{\text{stau}} \sim 100$ GeV we are able to get $0.0013 < c\tau$ (m) < 50 [$0.13 < c\tau$ (m) < 25] for the minimal track length of 1 cm (1 m) requirement. We also note that we are using a somewhat conservative integral luminosity of 50 fb^{-1} .

⁴We note that we used an almost pure right-handed stau that indeed gives a somewhat lower cross section than a left-handed stau.

Also in Fig. 5 is shown in dotted lines a 90% confidence level upper limit for $c\tau$, assuming that stau decays outside the detector. From Eq. (2) we can see that this value corresponds to a lower bound $\sqrt{F} \sim 1 \times 10^7$ GeV, which is slightly above cosmologically preferred value.

IV. CONCLUSIONS

In many supersymmetry scenarios a charged long-lived particle is predicted. For instance, in the GMSB scenario such particle would be a stau in a large portion of parameter space. We have studied the long-lived stau pair production in a linear collider at $\sqrt{s} = 500$ GeV. The linear collider will be able to study the stau pair where no other particles are produced in the event (except for beamsstrahlung, etc.), as opposed to the LHC where all supersymmetric reactions should be taken into account [13,10], being, in principle, a good place to extract the parameters of the model.

We presented in a model-independent way the minimal cross section for the pair production of stable nonstrongly interacting charged particle that will be observed in the NLC, considering just momentum measurement as well as particle identification devices. When the predicted cross section for the stau pair production in the GMSB model is considered it

is shown that the NLC will be able to detect such reactions for stau masses up to 85% of the beam energy, with just momentum measurement. Particle identification devices will extend the mass range to essentially the full beam energy. Moreover, particle identification devices will provide a sample of events essentially background free.

We also presented a way to extract the stau lifetime using the predicted cross section and a luminosity of 50 fb^{-1} . The method presented is very straightforward and does not depend on any other parameter of the model. For the range of masses that is possible to probe in a 500-GeV linear collider, the precision obtained is, in general, better than it will be possible to have from the LHC and it is mostly model independent.

ACKNOWLEDGMENTS

We thank X. Tata for valuable discussions and a careful reading of the manuscript. This work was supported by the U. S. Department of Energy under Contract Nos. DE-FG02-97ER41022 and DE-FG03-94ER40833. During his stay at the University of Hawaii where this work was started, P.G.M. was partially supported by Fundação de Amparo à Pesquisa do Estado de São Paulo (FAPESP).

-
- [1] N. V. Krasnikov, Phys. Lett. B **386**, 161 (1996).
 [2] J. L. Feng, T. Moroi, L. Randall, M. Strassler, and S. Su, Phys. Rev. Lett. **83**, 1731 (1999).
 [3] L. Randall and R. Sundrum, Nucl. Phys. **B557**, 79 (1999); T. Gherghetta, G. F. Giudice, and J. D. Wells, *ibid.* **B559**, 27 (1999); F. E. Paige and J. D. Wells, hep-ph/0001249.
 [4] M. Dine, W. Fischler, and M. Srednicki, Nucl. Phys. **B189**, 575 (1981); S. Dimopoulos and S. Raby, *ibid.* **B192**, 353 (1981); L. Alvarez-Guamé, M. Claudson, and M. Wise, *ibid.* **B207**, 96 (1982).
 [5] M. Dine and A. Nelson, Phys. Rev. D **48**, 1277 (1993); M. Dine, A. Nelson, and Y. Shirman, *ibid.* **51**, 1362 (1995); M. Dine, A. Nelson, Y. Nir, and Y. Shirman, *ibid.* **53**, 2658 (1996).
 [6] M. Drees and X. Tata, Phys. Lett. B **252**, 695 (1990).
 [7] S. Dimopoulos, M. Dine, S. Raby, and S. Thomas, Phys. Rev. Lett. **76**, 3494 (1996); S. Dimopoulos, S. Thomas, and J. Wells, Phys. Rev. D **54**, 3283 (1996); Nucl. Phys. **B488**, 39 (1997); S. Ambrosanio *et al.*, Phys. Rev. Lett. **76**, 3498 (1996); Phys. Rev. D **54**, 5395 (1996); K. S. Babu, C. Kolda, and F. Wilczek, Phys. Rev. Lett. **77**, 3070 (1996); H. Baer, M. Brhlik, C. H. Chen, and X. Tata, Phys. Rev. D **55**, 4463 (1997); J. Bagger, K. Matchev, and D. Pierce, *ibid.* **55**, 3188 (1997); R. Rattazzi and U. Sarid, Nucl. Phys. **B501**, 297 (1997); D. Dicus, B. Dutta, and S. Nandi, Phys. Rev. Lett. **78**, 3055 (1997); Phys. Rev. D **56**, 5748 (1997); K. Cheung, D. Dicus, B. Dutta, and S. Nandi, *ibid.* **58**, 015008 (1998); B. Dutta, D. J. Mueller, and S. Nandi, Nucl. Phys. **B544**, 451 (1999); D. J. Mueller and S. Nandi, Phys. Rev. D **60**, 015008 (1999); J. Feng and T. Moroi, *ibid.* **58**, 035001 (1998); E. Gabrielli and U. Sarid, *ibid.* **58**, 115003 (1998); S. Martin and J. Wells, *ibid.* **59**, 035008 (1999).
 [8] C. H. Chen and J. F. Gunion, Phys. Lett. B **420**, 77 (1998); Phys. Rev. D **58**, 075005 (1998).
 [9] See G. Giudice and R. Rattazzi, Phys. Rep. **322**, 419 (1999); **322**, 501 (1999), for a review.
 [10] H. Baer, P. G. Mercadante, F. Paige, X. Tata, and Y. Wang, Phys. Lett. B **435**, 109 (1998); H. Baer, P. G. Mercadante, X. Tata, and Y. Wang, Phys. Rev. D **60**, 055001 (1999); **62**, 095007 (2000); I. Hinchliffe and F. E. Paige, *ibid.* **59**, 035008 (1999).
 [11] DELPHI Collaboration, P. Abreu *et al.*, Eur. Phys. J. C **7**, 595 (1999).
 [12] See the web page: <http://lcwww.physics.yale.edu/lc/graphics.html>
 [13] S. Ambrosanio *et al.*, J. High Energy Phys. **01**, 014 (2001).
 [14] R. Culbertson *et al.*, hep-ph/0008070.
 [15] S. Ambrosanio and G. A. Blair, Eur. Phys. J. C **12**, 287 (2000).
 [16] See the web page: <http://www.cern.ch/Physics/LCWS99/talks.html>
 [17] P. G. Mercadante and H. Yamamoto, hep-ph/9909280.
 [18] H. Pagels and J. R. Primack, Phys. Rev. Lett. **48**, 223 (1982); T. Moroy, H. Murayama, and M. Yamaguchi, Phys. Lett. B **303**, 289 (1993); A. Masiero and M. Yamaguchi, *ibid.* **386**, 189 (1996); A. de Gouveia, T. Moroy, and H. Murayama, Phys. Rev. D **56**, 1281 (1997).
 [19] H. Baer, F. Paige, S. Protopopescu, and X. Tata, hep-ph/9810440.
 [20] P. Chen, Phys. Rev. D **46**, 1186 (1992).
 [21] Particle Data Group, C. Caso *et al.*, Eur. Phys. J. C **3**, 1 (1998).
 [22] BABAR Technical Design Report, SLAC-R-95-457, 1995.